

AFIP ARCHIVES

Best Cases from the AFIP

Supratentorial Ependymoma¹

Koen Mermuys, MD • Wino Jeuris, MD • Piet K. Vanhoenacker, MD • Lieven Van Hoe, MD, PhD • Pierre D'Haenens, MD

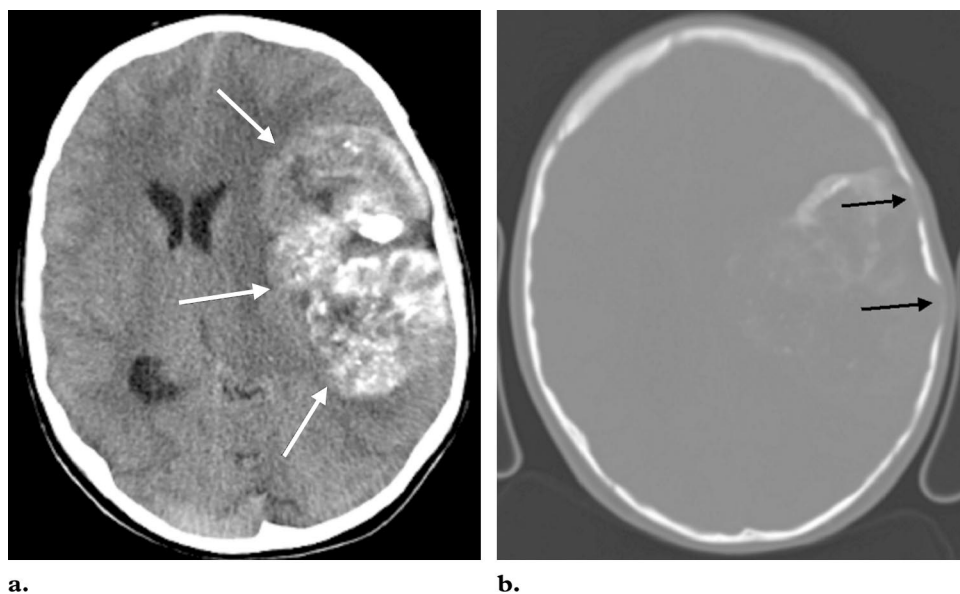


Figure 1. (a) Axial unenhanced CT scan of the brain shows a large (9.5×6 cm) space-occupying lesion in the left cerebral hemisphere (arrows) with mass effect and large internal calcifications. (b) Axial unenhanced CT scan of the brain (bone window) shows scalloping of the internal cortex of the parietal bone (arrows) and the calcifications in the tumor.

History

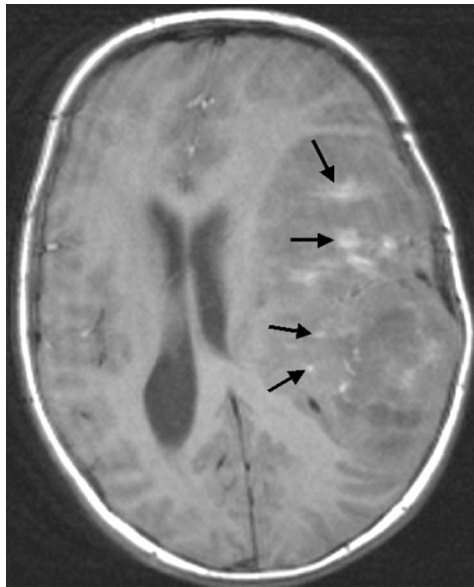
A 12-year-old boy presented with severe headache and acute onset of vomiting. The patient had a 6-year history of chronic headaches and had repeatedly been treated for sinusitis, with variable success. Physical neurologic examination showed a well-oriented patient with good coordination and normal reflexes. No laboratory abnormalities were noted. Results of chest radiography and electrocardiography were normal.

Imaging Findings

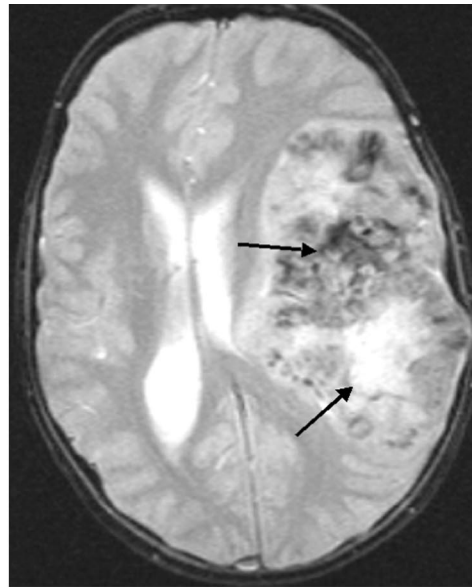
Initially, unenhanced computed tomography (CT) of the brain was performed. A large lesion (9.5×6 cm) was revealed in the left cerebral hemisphere. The lesion showed mass effect, large

internal calcifications, and scalloping of the internal cortex of the parietal bone (Fig 1).

Subsequently, magnetic resonance (MR) imaging was performed. On unenhanced T1-weighted images, the tumor was iso- to hypointense compared to the surrounding tissue and contained some small central hyperintense areas, which probably represented intratumoral hemorrhage (Fig 2a). On T2-weighted and fluid-attenuated inversion recovery (FLAIR) images, the tumor was heterogeneous with a striking lack of surrounding edema (Fig 2b, 2c). In the anterior portion of the tumor, T2-weighted images showed hypointense areas that represented calcifications. More posteriorly, hyperintense areas consistent with necrosis could be observed. On gadolinium-enhanced T1-weighted images, the tumor showed intermediate contrast



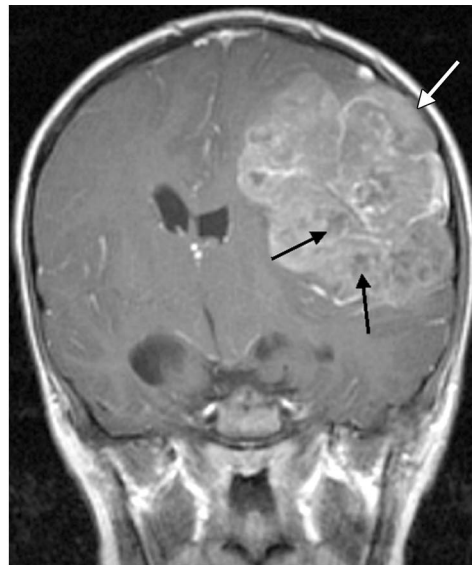
a.



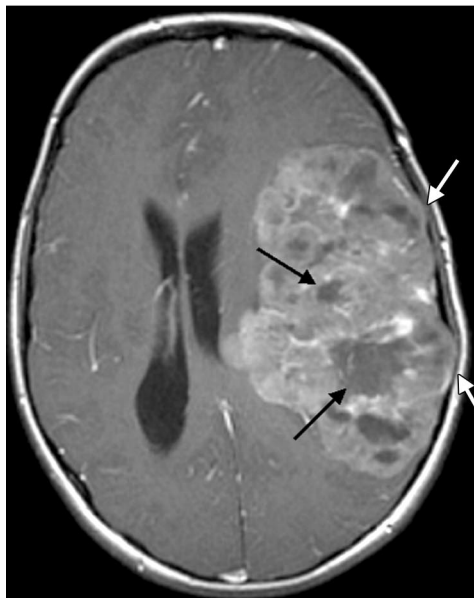
b.



c.



d.



e.

Figure 2. (a) Axial T1-weighted image shows that the tumor is iso- to hypointense. Arrows = hyperintense areas consistent with hemorrhage. (b) Axial T2-weighted image shows that the tumor is largely heterogeneous with hypointense areas representing calcifications (top arrow) and hyperintense areas consistent with necrosis (bottom arrow). (c) Axial FLAIR image shows that the tumor is moderately hyperintense with central areas of high signal intensity due to necrosis (arrows). (d, e) Coronal (d) and axial (e) gadolinium-enhanced T1-weighted images show moderate enhancement of the tumor with nonenhancing areas of necrosis (black arrows). White arrows = invasion of the overlying meninges and bone.

enhancement with multiple nonenhancing areas of necrosis, mainly in the posterior portion of the tumor (Fig 2d, 2e). There was invasion of the overlying meninges and scalloping of the internal cortex of the parietal bone.

Pathologic Evaluation

Surgical resection of the tumor was performed. The tumor had broken through the dura and had invaded the internal cortex of the parietal bone.

At gross examination of the resection specimen, the tumor was lobulated (size, $8 \times 5 \times 5$ cm; weight, 151 g) and the cut surface was soft and grayish red, with a few white necrotic foci and areas of hemorrhage (Fig 3). Furthermore, two rather distinct components could be identified: a clearly calcified posterior part and a soft and pink anterior part.

Histologic examination confirmed the lobular architecture and revealed a moderately cellular to paucicellular tumor with numerous dystrophic calcifications and multiple zones with necrosis or degeneration with fibrosis or hemorrhage (Fig 4a). The cytoplasm was eosinophilic and the nuclei were round and fairly uniform, most often with a finely distributed chromatin and small nucleoli. Mitotic figures were occasionally identified. The tumor was highly vascularized with numerous branching and thin-walled vessels, typically surrounded by acellular and fibrillar zones (pseudorosettes) (Fig 4b).

Discussion

Ependymomas are glial tumors derived from differentiated ependymal cells lining the ventricles of the brain and the central canal of the spinal cord (1,2). They are common neoplasms, constituting 3%–9% of all neuroepithelial neoplasms, 6%–12% of all pediatric brain tumors, and almost one-third of all brain tumors in patients younger than 3 years (3). Forty percent of ependymomas are supratentorial, while 60% are infratentorial in location (4). Ependymomas may manifest at any age (documented age ranges from 1 month to 81 years) with no gender predilection. The posterior fossa ependymoma arises most often in children (mean age, 6 years). The supratentorial ependymoma generally manifests in an older age group (mean age, 18–24 years) (3).

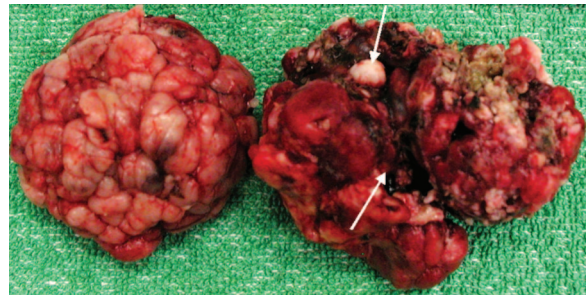


Figure 3. Photograph of the resected specimen shows that the tumor is lobulated with two fairly distinct areas: a soft, pink anterior component (left) and a posterior component (right) that clearly has areas of necrosis (top arrow) and hemorrhage (bottom arrow).

The supratentorial ependymoma has a different clinical and radiologic presentation than its infratentorial counterpart. The infratentorial ependymoma, due to its intraventricular location, will clinically manifest earlier secondary to increased intracranial pressure and hydrocephalus. Hydrocephalus nearly always occurs when an infratentorial ependymoma is present. This is not the case with the supratentorial ependymoma (5). Patients with supratentorial ependymomas tend to present with focal neurologic deficits, headache, and seizures (3).

Radiologically, the supratentorial ependymoma is more commonly seated in the brain parenchyma than the infratentorial ependymoma, which is more often located intraventricularly (5,6). Swartz et al (7) reported that 83% of supratentorial ependymomas are located in the cerebral parenchyma. It is speculated that ependymomas may arise from embryonic rests of ependymal tissue trapped in the developing cerebral hemispheres (3). Owing to its parenchymal location, the supratentorial ependymoma tends to be larger in size than its infratentorial counterpart. Arming-ton et al (5) found that 94% of supratentorial tumors manifest with a size larger than 4 cm, while most infratentorial ependymomas are significantly smaller at presentation. Supratentorial ependymomas often contain a cystic component, while infratentorial ependymomas are often more solid tumors (5,8). Calcification, ranging from small punctate foci to large masses, is very common in both infra- and supratentorial ependymomas (40%–80% of cases) (3,8). In this case, there was no cystic component.

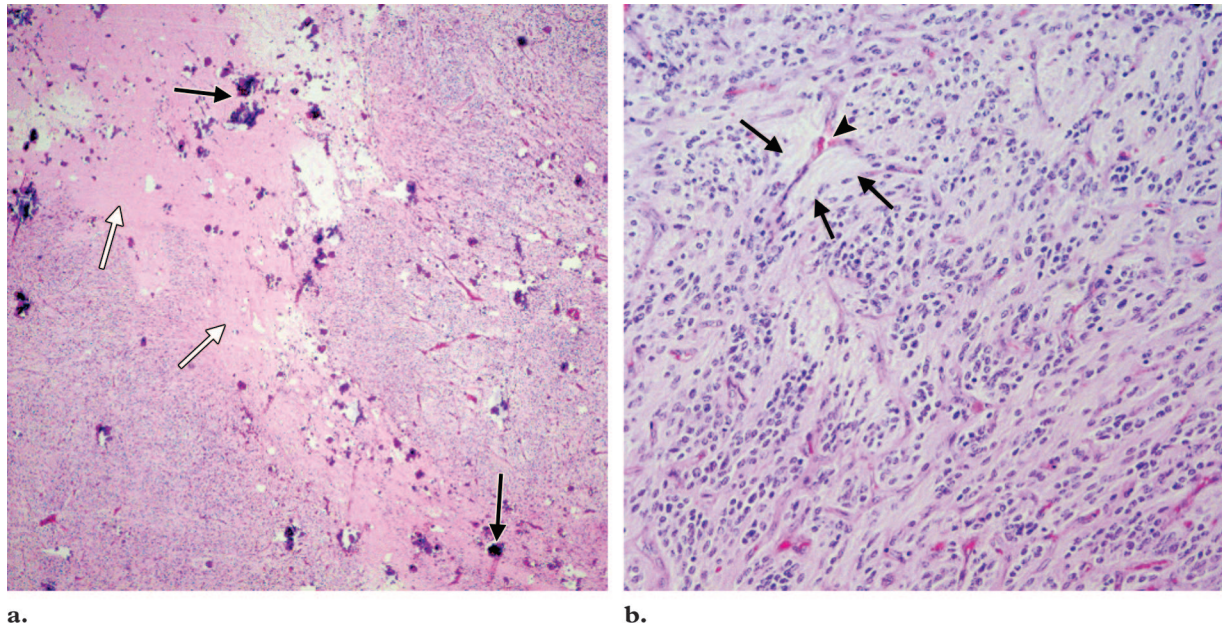


Figure 4. (a) Low-power photomicrograph (original magnification, $\times 40$; hematoxylin-eosin stain) shows that the tumor is moderately cellular with necrotic and fibrotic transformed areas (white arrows) and numerous dystrophic calcifications (black arrows). (b) High-power photomicrograph (original magnification, $\times 200$; hematoxylin-eosin stain) shows that the tumor is moderately cellular and highly vascularized with numerous branching thin-walled vessels (arrowhead). Some of the vessels are typically surrounded by a fibrillar and acellular zone (pseudorosettes) (arrows).

Infratentorial and supratentorial ependymomas have the same imaging characteristics at CT and MR imaging. The lesions are iso- to slightly hypoattenuating to surrounding normal brain tissue at unenhanced CT (2,5,6,8). They are iso- to hypointense relative to normal white matter on unenhanced T1-weighted MR images and hyperintense on T2- and proton-density-weighted MR images. Foci of signal heterogeneity within a solid neoplasm represent methemoglobin, hemosiderin, necrosis, or calcification (4,6). Ependymomas can display variable contrast enhancement behavior but generally enhance moderately intensely at both CT and MR imaging, with central areas of necrosis (1,2,5). The differential diagnosis for lesions with the appearance of an extraventricular supratentorial ependymoma should include astrocytoma (both low grade and glioblastoma multiforme), supratentorial primitive neuroectodermal tumor, ganglioglioma-cytoma, and oligodendroglioma (4,5,7).

At histologic analysis, ependymomas are moderately cellular tumors with rare mitotic figures. The tumor cells are characteristically organized in

perivascular pseudorosettes and, less commonly, ependymal rosettes. They are considered World Health Organization (WHO) grade II lesions (3).

The 5-year progression-free rate for children overall is about 50%. The 5- and 10-year survival rates for adults are 57.1% and 45%, respectively (3,9). There are three major factors that were found to have a significant impact on outcome. The presence of radiologic residual disease, seen at postoperative MR imaging or CT, is the most important prognostic variable. Of patients with no radiologic evidence of residual tumor, $75\% \pm 15\%$ will remain tumor free after 5 years as opposed to the group of patients with residual disease in which progression cannot be stopped (10). Age at presentation is also a significant prognostic factor (10). Patients younger than 3 years have a significantly worse outcome than older children (9–11). The last prognostic variable is the duration of symptoms before diagnosis. Patients with a duration of symptoms before diagnosis of less than 1 month have a worse outcome than those

with a more protracted course (9). In general, patients with supratentorial ependymomas have a better survival rate than patients with posterior fossa ependymomas (3,11).

The treatment of choice is total radical resection. Radical surgery alone is a reasonable option as the initial treatment for solid extraventricular tumors located far from clinically eloquent brain areas. Postoperative radiation therapy must be administered in every case of partially resected ependymomas as well as for those extraventricular ependymomas that are cystic or located near eloquent brain areas, even after apparently total resection. The "prophylactic" use of spinal irradiation is not necessary in supratentorial ependymomas of children and young adults.

The patient in this case was treated with radical tumorectomy and postoperative radiation therapy. There was no evidence of residual tumor at postoperative imaging. The patient had an uneventful recovery and was discharged. After 9 months, the patient was tumor free at clinical and radiologic examination.

References

1. Furie DM, Provenzale JM. Supratentorial ependymomas and subependymomas: CT and MR appearance. *J Comput Assist Tomogr* 1995; 19:518–526.
2. Osborn AG, Daines JH, Wing SD. The evaluation of ependymal and subependymal lesions by cranial computed tomography. *Radiology* 1978; 127:397–401.
3. Koeller KK, Sandberg GD. Cerebral intraventricular neoplasms: radiologic-pathologic correlation. *RadioGraphics* 2002; 22:1473–1505.
4. Spoto GP, Press GA, Hesselink JR, et al. Intracranial ependymoma and subependymoma: MR manifestations. *AJR Am J Roentgenol* 1990; 154:837–845.
5. Armington WG, Osborn AG, Cubberley DA, et al. Supratentorial ependymoma: CT appearance. *Radiology* 1985; 157:367–372.
6. McConachie NS, Worthington BS, Cornford EJ, et al. Review article: computed tomography and magnetic resonance in the diagnosis of intraventricular cerebral masses. *Br J Radiol* 1994; 67:223–243.
7. Swartz JD, Zimmerman RA, Bilaniuk LT. Computed tomography of intracranial ependymomas. *Radiology* 1982; 143:97–101.
8. Morrison G, Sobel DF, Kelley WM, et al. Intraventricular mass lesions. *Radiology* 1984; 153:435–442.
9. Pollack IF, Gerszten PC, Martinez AJ, et al. Intracranial ependymomas of childhood: long-term outcome and prognostic factors. *Neurosurgery* 1995; 37:655–666.
10. Healey EA, Barnes PD, Kupsky WJ, et al. The prognostic significance of postoperative residual tumor in ependymoma. *Neurosurgery* 1991; 28:666–671.
11. Kudo H, Oi S, Tamaki N, et al. Ependymoma diagnosed in the first year of life in Japan in collaboration with the International Society for Pediatric Neurosurgery. *Childs Nerv Syst* 1990; 6:375–378.